DC Actuators and their Operation Characteristics

IVO DOLEŽEL, PAVEL DVOŘÁK, BOHUŠ ULRYCH
National Center "New Technologies"
Faculty of Electrical Engineering, University of West Bohemia
Univerzitní 8, 306 14 Plzeň
Czech Republic

Abstract: – DC actuators belong to devices frequently used in a lot of industrial applications. Their spectrum is considerably wide and ranges from small units in robotics and various control systems to heavy drive systems for rods in nuclear reactors. But despite their simple construction, numerical simulation of their behavior and optimization of their parameters and characteristics is relatively difficult due to the presence of non-linear materials and movable parts. In case of highly exposed devices, moreover, even thermal and mechanical effects have to be taken into account. The paper summarizes techniques suitable for their mathematical and computer modeling and illustrates them on several typical examples whose results are discussed.

Key-Words: – DC actuators, electromagnetic field, temperature field, numerical analysis

1 Introduction

Linear drive systems with DC electromagnets play an important role in various industrial processes, control systems, robotics and a lot of other applications. One of their typical features is simple construction and highly reliable functioning. On the other hand, determination and optimization of their parameters and characteristics in the stage of design is a relatively difficult business due to the presence of non-linear materials (ferromagnetics, permanent magnets) and movable parts. That is why more and more sophisticated models and corresponding numerical algorithms are developed and used for analysis and evaluation of these quantities, particularly in case of smaller units where very high accuracy is required.

The basic task to be solved is finding the static (and eventually dynamic) characteristic. Techniques of their determination have been improved for a long time (see, for example, [1] and [2]) and nowadays they can be declared robust and reliable. More complicated and not fully analyzed are, however, thermal phenomena. Nevertheless, even solution of coupled problems of this kind can be realized by suitable professional codes extended by supplementary single-purpose user procedures [3] and [4].

The paper summarizes existing methods for solving complete mathematical models of the devices developed by the authors and illustrates them on typical examples whose results are discussed.

2 Technical aspects of the problem

As known, DC electromagnets can work in short-term and long-term operation regimes. For short-term regimes the most important quantities are usually the shape of the static characteristic and sometimes also dynamic parameters (pull-in velocity and time). On the other hand, long-term regimes are often limited by temperature rise of the system due to the Joule losses produced by the field current. Thermal effects have to be considered, however, even in shorter transients when the field current is high.

All the mentioned characteristics are functions of the arrangement of the device, geometry of its structural parts, way of cooling etc. The number of the degrees of freedom affecting operation of the device is, therefore, not low and optimization of the design cannot be carried out directly. Thus, the usual way starts from an existing device with similar parameters and its consequent modification leading to required operation properties.

The authors freely collaborate with one of the Czech manufacturers (company LEKOV) and several users of the devices. They belong to experienced experts in the field and deal even with nonstandard tasks. They published a number of papers in the domain, suggested several original algorithms for mapping transients and steady states and solved a lot of problems concerning the design of particular systems.

3 Mathematical model and its solution

The basic mathematical model of the device generally consists of two nonlinear partial differential equations describing distribution of electromagnetic and temperature fields and two nonlinear ordinary differential equations describing transients in the feeding electrical and mechanical circuits. A simplified schematic

axisymmetric arrangement of the device is depicted in Fig. 1.

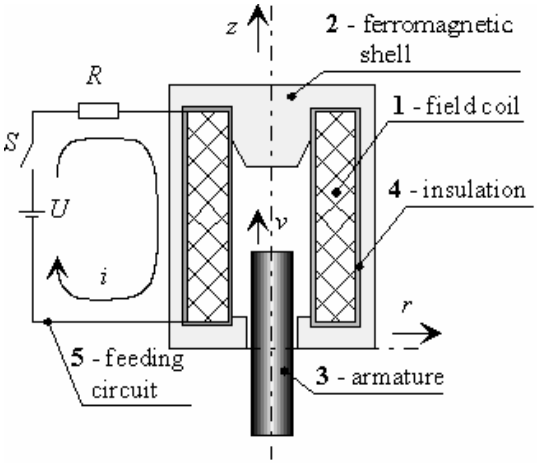

Fig. 1: A simplified arrangement of the device

At the moment when the field coil **1** is connected to the voltage source, the time-dependent current i starts producing magnetic field and due to the Maxwell forces the armature **3** is pulled into the device. At the same time, the Joule losses generated in the coil (and, exactly, also in other electrically conductive parts) begin to heat the system.

As mentioned before, the device can work in the *short-term* or *long-term* regime and its field coil can be supplied either from a *voltage source* or from a *current source*. All four possible combinations are generally described by different mathematical models discussed later on.

In case of voltage source the field current i is a time variable quantity whose evolution follows from equation

$$\left(R+R_{\mathrm{c}}\right)i+\frac{\mathrm{d}}{\mathrm{d}t}\left(Li\right)=U \qquad (01)$$

where R is the resistance of the feeders, R_{c} the resistance of the coil and L the total inductance of the system that is (due to material nonlinearities and movement of the armature) a function of current i and position z. The initial condition reads $i(0)=0$. The value of inductance L is given as

$$L=\frac{2W}{i^2} \qquad (02)$$

where W is the magnetic field energy that may be determined from magnetic field distribution.

Electromagnetic field in the system can be described in terms of vector potential $\boldsymbol{A}$. Its distribution in short-term regimes is generally given by equation

$$\mathrm{rot}\left(\left[\mu\right]^{-1}\mathrm{rot}\,\boldsymbol{A}\right)+\gamma\frac{\mathrm{d}\boldsymbol{A}}{\mathrm{d}t}=\boldsymbol{j}_{\mathrm{ext}} \qquad (03)$$

where magnetic permeability μ may be nonlinear and anisotropic, γ is the electrical conductivity and $\boldsymbol{j}_{\mathrm{ext}}$ the time-dependent vector of density of the field current i. Boundary conditions to this equation depend on the solved arrangement.

In long-term regimes, however, influence of eddy currents produced in electrically conductive structural parts (that are respected by the second term on the left side of (03)) may be neglected because of very short time of the transient, practically without any consequent heating effects. Then we can replace (03) by simpler equation

$$\mathrm{rot}\left(\left[\mu\right]^{-1}\mathrm{rot}\,\boldsymbol{A}\right)=\boldsymbol{J}_{\mathrm{ext}} \qquad (04)$$

where $\boldsymbol{J}_{\mathrm{ext}}$ is the steady-state current density.

If the coil is supplied from the current source (characterized by constant current I), then the field distribution is always given by (04).

Distribution of magnetic field is also the starting point for computation of the total force $\boldsymbol{F}_{\mathrm{m}}$ acting on the movable parts of the device. This quantity can be obtained from the Maxwell tensor and its value is given by formula

$$\boldsymbol{F}_{\mathrm{m}}=\frac{1}{2}\cdot\oint_{S_{\mathrm{m}}}\left[\boldsymbol{H}\left(\boldsymbol{n}\cdot\boldsymbol{B}\right)+\boldsymbol{B}\left(\boldsymbol{n}\cdot\boldsymbol{H}\right)-\boldsymbol{n}\left(\boldsymbol{H}\cdot\boldsymbol{B}\right)\right]\mathrm{d}S \qquad (05)$$

where S_{m} denotes the whole surface of these movable parts **3**, $\boldsymbol{B}$ and $\boldsymbol{H}$ are the field vectors along this surface and $\boldsymbol{n}$ the unit vector of its outward normal.

Movement of the movable parts during the mechanical transient is described by nonlinear equation

$$m_{\mathrm{m}}\cdot\frac{\mathrm{d}\boldsymbol{v}}{\mathrm{d}t}=\boldsymbol{F}_{\mathrm{m}}-\boldsymbol{F}_{\mathrm{fr}}-\boldsymbol{F}_{\mathrm{ot}},\ \boldsymbol{v}=\frac{\mathrm{d}\boldsymbol{z}}{\mathrm{d}t} \qquad (06)$$

where m_{m} is their total mass, $\boldsymbol{v}=\boldsymbol{v}(t)$ their velocity, $\boldsymbol{F}_{\mathrm{fr}}$ the friction (resistance of the medium) and $\boldsymbol{F}_{\mathrm{ot}}$ other forces (whose consideration depends on the case investigated; in some cases, for example, gravitational force may play a significant role). Suppose that (in accordance with Fig. 1) the armature moves in direction z. Then all forces in (06) have only one component in the same direction and the following inequalities hold

$$\begin{aligned} F_{\mathrm{m},z}\le F_{\mathrm{pas},z}\Rightarrow v_z=0 \text{ and } F_{\mathrm{fr}}=0,\\ F_{\mathrm{m},z}\ge F_{\mathrm{pas},z}\Rightarrow v_z>0 \text{ and } F_{\mathrm{fr}}=f(v_z)>0 \end{aligned} \qquad (07)$$

where $F_{\mathrm{pas},z}$ denotes the passive resistance of the mechanism. In other words, after turning on the switch an increasing electromagnetic force $F_{\mathrm{m},z}$ starts to act on the armature in direction z. As soon as this force exceeds the passive resistance $F_{\mathrm{pas},z}$ of the mechanism, the armature begins to move at acceleration a_z and velocity v_z. At this moment force $F_{\mathrm{pas},z}$ vanishes and new velocity-dependent drag force F_{fr} appears.

The nonstationary temperature field in the system is described by equation

$$\operatorname{div}\left(\lambda \operatorname{grad} T\right) = \rho c \cdot \frac{\partial T}{\partial t} - w_0 \qquad (08)$$

where λ denotes the thermal conductivity, ρ and c the specific mass and heat, respectively, and w_0 the specific Joule losses representing the sources of heat. These losses are generally supposed to be produced within the field coil

$$w_0 = \frac{R_\mathrm{c} \cdot i^2}{V_\mathrm{c}} \qquad (09)$$

where V_c is its volume and also in other electrically conductive structural parts (during transients)

$$w_0 = \gamma \left(\frac{\mathrm{d}A}{\mathrm{d}t} \right)^2 . \qquad (10)$$

More detailed computations can also respect the temperature dependencies (as far as they are significant) of material parameters γ, λ, ρ, c and μ.

The boundary conditions have to be imposed according to properties of the arrangement. Heat transfer from the shell **2** may be realized by convection and radiation, taken into account may also be forced cooling of the field coil etc.

Beside the above mathematical models for common devices, sometimes we have to build even more sophisticated models. These are, however, quite individual and depend on the solved arrangement.

As far as the authors know, a complete general model consisting of equations (01), (02), (05), (06) and (08) cannot be solved by any existing professional code. Some of them (ANSYS, Femlab) would perhaps allow relatively sophisticated computations, but not without considerable programmer's work supplementing their pre-programmed possibilities. Even more complicated would be solution of even more complex models (that respect, for example, temperature dependencies of the material parameters). It turns out that probably the most advantageous way is to use suitable commercial codes for evaluating particular physical fields and write own procedures for solution of both circuit equations.

4 Illustrative examples

The authors successfully designed, solved and optimized a lot of particular arrangements that are now used in various industrial applications. In the next text two of them will be described in more details.

4.1 An actuator for aggressive environment

Investigated is an axisymmetric electromagnet designed for operation in chemically active environment containing SO_2 (Fig. 2). Its magnetic circuit from non-linear iron is protected by outer shell from austenitic, chemically stable non-ferromagnetic steel.

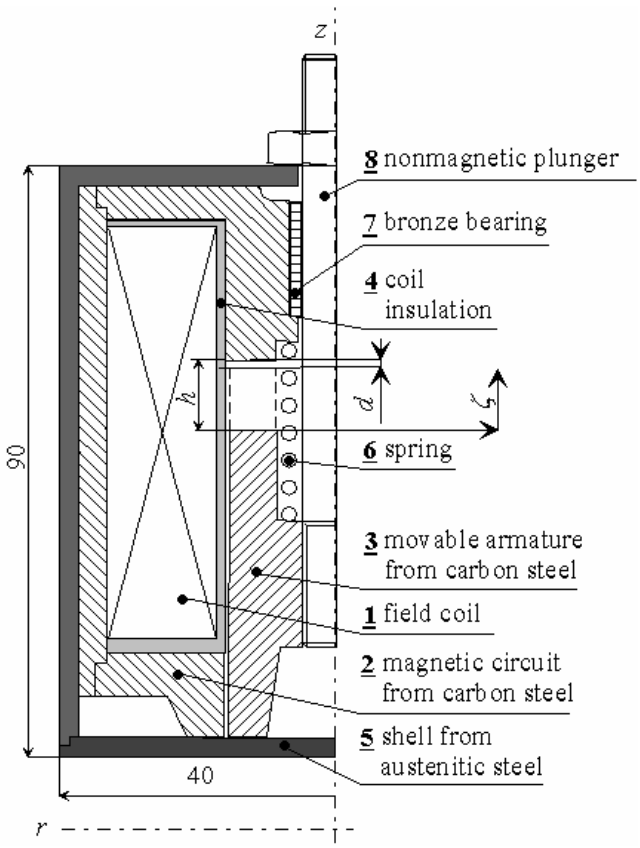

Fig. 2: Disposition of the actuator (in the switched-on regime the armature is in position *d*)

The field coil **1** fed from a current source with Teflon insulation **4** is placed inside hollow ferromagnetic shell **2** screwed together from three parts. Ferromagnetic armature **3** of the actuator is connected with the external mechanism by austenitic (nonferromagnetic) rod **8** passing through a bronze friction bearing **7**. Spring **6** returns (after switching off the field current) the armature with rod from the switch-on position d to the starting switch-off position h. The whole system is placed in chemically stable austenitic nonferromagnetic shell **5**. The actuator is supposed to prevailingly operate in the switch-on state with current I_ext.

The most important geometrical and electric parameters of individual parts follow:

- Field coil **1**: wound by enameled Cu wire (diameter $d = 1.075$ mm), number of turns $N_\mathrm{c} = 780$, volume $V_\mathrm{c} = 1.414 \cdot 10^{-4}$ m^3, coefficient of filling $k_\mathrm{f} = 0.68$, resistance $R_\mathrm{c} = 9.964\,\Omega$, modified (with respect to the coefficient of filling) thermal conductivity $\lambda = 268.6$ W/mK and heat capacity $\rho c = 2.5 \cdot 10^6$ J/m^{3}K. The coil carries current I_ext.

- Ferromagnetic circuit **2** and armature **3** (carbon steel 12 040): average values of thermal conductivity and heat capacity are $\lambda = 48.0$ W/mK and $\rho c = 3.9 \cdot 10^6$ J/m^{3}K, respectively.
- Austenitic shell **5** and rod **8** (steel 17 335): relative permeability μ_r = 1, average values of thermal conductivity and heat capacity are $\lambda = 15.0$ W/mK and $\rho c = 4.2 \cdot 10^6$ J/m^{3}K, respectively.
- Insulation **4** made from Teflon, $\lambda = 0.23$ W/mK, $\rho c = 2.4 \cdot 10^6$ J/m^{3}K, maximum permissible temperature $T_{\mathrm{p\,max}} = 200$ °C.
- Bronze bearing **7**: $\lambda = 42.0$ W/mK, $\rho c = 2.1 \cdot 10^6$ J/m^{3}K.

Investigated was temperature rise of the actuator in steady state pull-in regime for varying field currents. Current for which the maximum temperature reaches the highest possible value $T_{\max} = T_{\mathrm{p\,max}} = 200$ °C is $I_{\mathrm{nom}} = 3.257$ A.

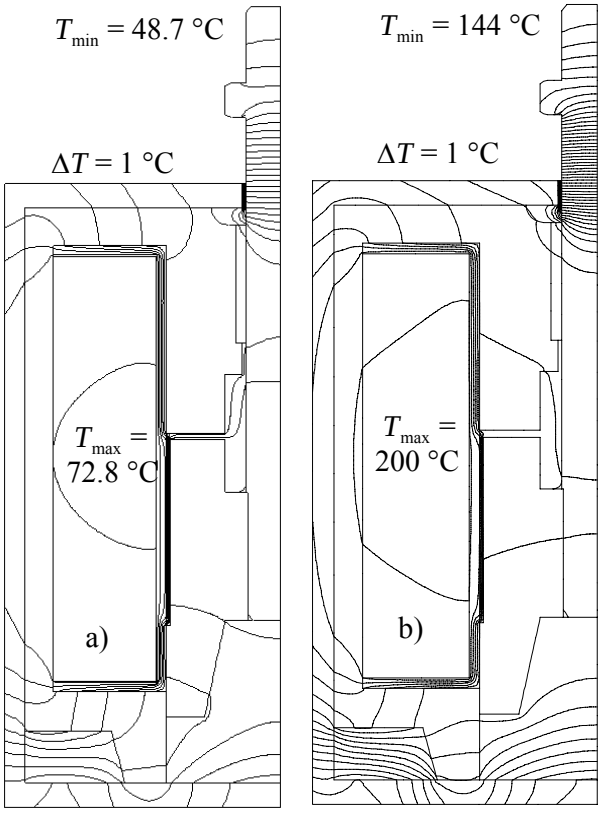

Fig. 3: Temperature field within the electromagnet for $I_{\mathrm{ext}} = I_{\mathrm{nom}}$ at time levels a) $t = 1200$ s, b) $t = \infty$

Distribution of the nonstationary temperature field within the device for time level $t = 1200$ s and current $I_{\mathrm{ext}} = I_{\mathrm{nom}}$ is shown in Fig. 3a. Fig. 3b depicts the stationary temperature field for the same parameters. As the fields are relatively uniform, there is no danger of larger thermoelastic displacements in the structural parts. Higher temperature gradient can be observed only in the field coil insulation **4**, inside external austenitic shell **5** and, particularly, at the place where austenitic rod **8** leaves the electromagnet. This is caused by an intensive contact with external cooling medium (a mixture of SO_2 and air of temperature $T_{\mathrm{ext}} = 30$ °C, convective heat transfer coefficient $\alpha = 40$ W/m^{2}K).

Fig. 4 shows the dependence of t_{200} (the time, when maximum temperature $T_{\max}$ of the system reaches value $T_{\mathrm{p\,max}} = 200$ °C) and also pull-in force $F_{\mathrm{m},z}$ in the switch-on position on field current I (related to current I_{nom}).

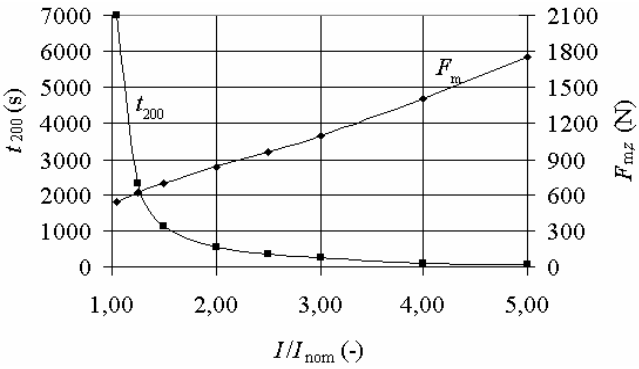

Fig. 4: Dependence of the time t_{200} of the switch-on regime and corresponding magnetic force $F_{\mathrm{m},z}$ acting on the armature on ratio I / I_{nom}

As can be seen in Fig. 4, the characteristic $t_{200}(I / I_{\mathrm{nom}})$ is strongly non-linear, which is caused by the quadratic dependence of specific losses w_0 (representing the source of heat) on current I. Unlike that, the dependence of force $F_{\mathrm{m},z}$ on I grows practically linearly.

4.2 An actuator combined with pulse induction accelerator

In some applications (circuit breakers etc.) the initial force acting on the armature should reach as high value as possible while ending of its movement should be rather slow in order to avoid hard impact. Such demands may be met by using of a device that combines properties of both the classic ferromagnetic actuator and pulse induction accelerator (Fig. 5).

After switching the upper circuit the condenser battery starts discharging and field coil **1** carrying current of the pulse character generates corresponding magnetic field. This field induces eddy currents in the ring **3** shifted by almost 180° from the field current. The force interaction between both these currents brings about movement of the ring in the direction of

axis z. Parameters (acceleration, velocity) of this movement may in wide extent be controlled by the lower circuit. At its beginning the force due to the mentioned interaction is enlarged (the ferromagnetic core is drawn into field coil **2**) while the same effect will later cause its reduction.

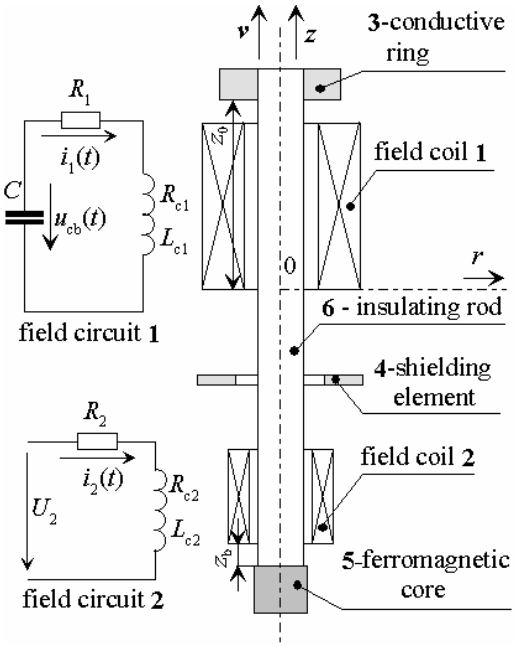

Fig. 5: Disposition of the combined actuator

Investigated is the dynamic characteristic of the device and time dependence of several other quantities such as currents, forces, acceleration and velocity of the movable parts during the transient. Unlike the basic mathematical model presented in chapter **3** we have to consider two more equations. The first one describes the time evolution of current $i_1(t)$ in the field circuit **1** and reads

$$u_{\mathrm{cb}}(0)-\frac{1}{C}\cdot\int_0^t i_1(\tau)\,\mathrm{d}\tau=(R_{\mathrm{c1}}+R_1)\cdot i_1(t)+\frac{\mathrm{d}L_{\mathrm{c1}}i_1(t)}{\mathrm{d}t} \quad (11)$$

where L_{c1} is a time-dependent quantity because of increasing distance between the field coil **1** and conductive ring **3**. The initial condition reads $i_1(0)=0$.

The second equation is for the electromagnetic force $F_{\mathrm{elm},z}$ (that is also a function of time) acting between the field coil **1** and ring **3** that has to be added to equation (06). This force follows from formula

$$F_{\mathrm{elm},z}=-\int_{V_{\mathrm{r}}} j_{\mathrm{r},\varphi}\cdot B_r\,\mathrm{d}V \quad (12)$$

where $j_{\mathrm{r},\varphi}$ is the eddy current density in the ring (that has only one component in the tangential direction) and B_r the radial component of magnetic flux density produced by coil **1** (which can be calculated from the Biot-Savart law). Integration is carried out over the whole ring **3**.

Provided that the arrangement is axisymmetric, both quantities L_{c1} and $F_{\mathrm{elm},z}$ may be calculated in a semianalytical way [5].

Computations have been performed on several arrangements. The principal data of one of them follow.

- Coil **1** (copper wire): inner radius $0.04\,\mathrm{m}$, outer radius $0.05\,\mathrm{m}$, height $0.10\,\mathrm{m}$, number of turns 1000, cross-section of the turn $10^{-4}\,\mathrm{m}^2$, total resistance of the coil $4.245\,\Omega$.
- Ring **3** (copper turn): inner radius $0.02\,\mathrm{m}$, outer radius $0.03\,\mathrm{m}$, height $0.01\,\mathrm{m}$, starting position $z_0=0.105\,\mathrm{m}$, mass $0.135\,\mathrm{kg}$.
- Coil **2** (copper wire): inner radius $0.015\,\mathrm{m}$, outer radius $0.02\,\mathrm{m}$, height $0.015\,\mathrm{m}$.
- Ferromagnetic core **5** (iron ČSN 12030): outer radius $0.01\,\mathrm{m}$, height $0.015\,\mathrm{m}$, mass $0.038\,\mathrm{kg}$.
- Condenser: $C=2\,\mathrm{mF}$, $u_{\mathrm{cb}}(0)=2500\,\mathrm{V}$.
- Length of the insulating Teflon rod **6**: $0.25\,\mathrm{m}$, mass of rod **6** $0.040\,\mathrm{kg}$.
- $z_{\mathrm{b}}=0.008\,\mathrm{m}$ (Fig. 6).

The movable part moves in the direction of axis z and the length of the trajectory is $0.015\,\mathrm{m}$. At this moment the movement stops and the feeding circuits are turned off.

The calculations were carried out by combination of program QuickField (distribution of the magnetic field of coil **2** with core **5** and determination of the corresponding inductance $L_{\mathrm{c2}}(t)$ and forces $F_{\mathrm{m},z}(t)$ and a single-purpose user program developed and written by the authors in Borland Pascal for complete evaluation of influence of electric circuit **1** and solution of the movement equations. Two variants have been computed and compared: the first one considers only coil **1** with the copper ring without the rod (electromagnetic accelerator), the second one also respects the influence of coil **2** with the ferromagnetic core and insulating rod. The computing time may range from several minutes to several hours.

The principal results are depicted in several following figures. Fig. 6 shows the time evolution of current i_1 flowing in the circuit **1** and total eddy currents i_{r} passing through ring **3**. While current i_1 grows with decreasing derivative, current i_{r} (that is shifted practically by 180°) reaches its maximum (with respect to its amplitude) at $t=0.0025\,\mathrm{s}$. After that, because of growing distance of ring **3** from the field coil **1**, its value decreases. The time in which the considered trajectory of $0.015\,\mathrm{m}$ is overcome reaches in both cases about $0.006-0.007\,\mathrm{s}$. That is why coil **1** and ring **3** satisfy also the temperature requirements

even when both currents (and, consequently, their densities) reach relatively high values.

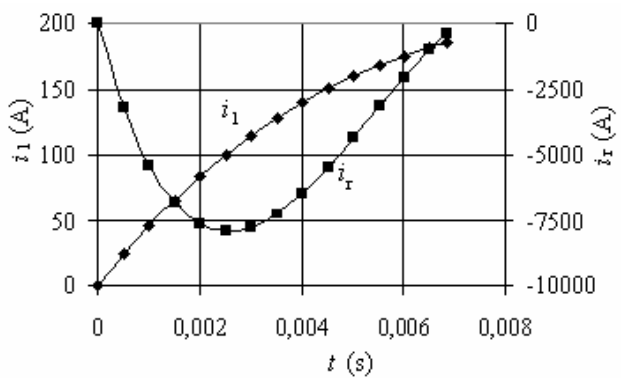

Fig. 6: Time evolution of currents i_1 and i_r

Fig. 7 shows the time evolution of voltage u_c on coil **1** and total electromagnetic force $F_z(t)$ acting on the movable part. This force includes both force $F_{elm,z}(t)$ acting on the ring and force $F_{m,z}(t)$ acting on the ferromagnetic core. While voltage u_c permanently decreases with growing current i_1, total electromagnetic force $F_z(t)$ approximately copies (see Fig. 6) the waveform of current i_r.

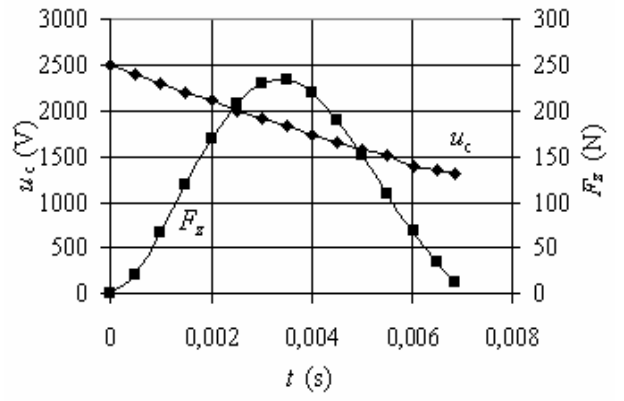

Fig. 7: Time evolution of u_c (voltage on field coil **1**) and total force F_z acting on movable parts

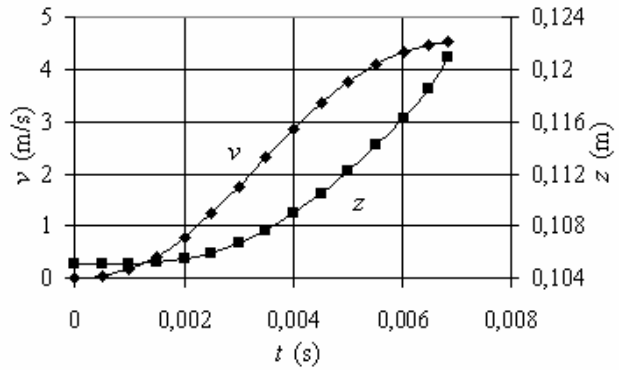

Fig. 8: Time evolution of velocity v and trajectory z of the movable part

Finally Fig. 8 shows the time evolution of velocity v_z and trajectory z of the movable part that varies from value $z_0 = 0.105\,\text{m}$ to value $0.120\,\text{m}$. Observable is damping of the velocity at the end of the movement.

5 Conclusion

Even when DC actuators belong to well explored devices and much is known about methodology of their design, there exist some domains that still deserve to be investigated in more details. Interesting are mainly limit transients and steady-state regimes (where thermal viewpoints play the decisive role) and also non-standard or non-traditional constructions.

In the area of non-standard designs the authors designed and optimized, for example, a large device for drive of rods in nuclear reactors (length of the device exceeding 3 m), special actuator for extremely high pull-in force whose field coil is wound by a hollow copper conductor cooled by water, device with almost flat static characteristic etc.

Planned is research of some other non-traditional designs (actuators based on the principle of thermoelasticity).

6 Acknowledgment

This work has been supported by the Ministry of Education of the Czech Republic (project of research and development LN 00 B084).

References:

[1] D. Mayer, B. Ulrych: Analysis of Transient State of Nonlinear Electromagnetic Actuator with Help of Professional SW. *Journal of Electrical Engineering*, Vol. 49, 1998, pp. 326–330.

[2] I. Doležel, M. Škopek, B. Ulrych: Operation Characteristics of a Cylindrical Electromagnetic Actuator with Permanent Magnet Core. *Proc. IC SPETO'99*, Ustroň, Poland, 1999, pp. 171–174.

[3] J. Barglik, I. Doležel, P. Dvořák, B. Ulrych, M. Škopek: Limit Operation Regimes of DC Actuator-Based Linear Drives. *Proc. IC ZKWE'03*, Poznaň, Poland, 2003, pp. 181–184.

[4] I. Doležel, P. Dvořák, B. Ulrych, J. Barglik: Transient Electromagnetic-Thermal Analysis and Optimisation of a DC Actuator-Based Linear Drive. *Proc. IC ISTET'03*, Warszawa, Poland, 2003, pp. 309–312.

[5] I. Doležel, M. Jaskovská, M. Škopek, B. Ulrych: Dynamic Characteristics of Combined Actuators. *Electromagnetic Fields in Electr. Engineering*. Warsaw University Press, 2002, pp. 401–406.